JTTEES 6:235-241

Determination of Residual Stress Distribution from in situ Curvature Measurements for Thermally Sprayed WC/Co Coatings

H. Liao, P. Vaslin, Y. Yang, and C. Coddet

An in situ monitoring of curvature of the specimen during spraying using a high speed video system was implemented to determine stresses in thermally sprayed WC/Co coatings. Influences of different spraying techniques (atmospheric plasma spraying and high-velocity oxygen fuel) and cooling levels were considered using a mathematical model. Results show that temperature history of a part is of paramount importance in stress generation and distribution.

Keywords curvature measurement, high speed video, residual stresses, stress distribution, tungsten carbide coating

1. Introduction

THERMAL SPRAYING is often used to deposit coatings for wear resistance applications; for example, coatings of tungsten carbide in a cobalt matrix are used due to high hardness and toughness.

However, WC/Co coatings may crack or spall from the substrate during or after thermal spraying because of stresses generated during the fabrication process. These stresses, which also determine various properties of the coating such as resistance to abrasion, are influenced not only by material properties but also by thermal spraying parameters. Thus, understanding, predicting, and reducing the level of residual stresses in coatings is an important technological aim. Stresses in coatings deposited by thermal spraying may induce deformation of the specimen if the specimen is thin enough. If it is possible to measure the deformation, the curvature for example, the value of these stresses can then be estimated.

Two main techniques can be used to measure the curvature of specimens. Measurement of the final curvature occurs after processing of the sample. Using this method, estimation can be made qualitatively (Ref 1) with calculations of the final residual stress on the coated surface (Ref 2). This method is useful to optimize thermal spray parameters, but it does not allow discrimination between various origins of stress. The second technique is continuous in situ measurement of the curvature. In this method, the curvature is continuously recorded during spraying. Therefore, the distribution of the stress (Ref 3), especially distribution of the quenching stress (stress produced in the splats upon cooling from melting point to the substrate temperature), can be analyzed (Ref 4). Measurements are made with a displacement sensor (Ref 4) or a video camera (Ref 3). Usually, during measurements, the specimen is fixed, and the spray gun is scanned. It is, therefore, difficult to follow optimum or usual kinematic parameters (100 mm · s^{-1}, for example, against 1250 mm · s^{-1} for the relative linear velocity of the torch across the substrate). In this work, the authors used a mobile specimen to reach the usual relative velocities of the torch with respect to the substrate and a high speed video system for continuously recording the curvature of the sample during spraying. Calculation of the stresses in the coating and the substrate through-thickness was then possible at different stages of the spraying process.

H. Liao, Y. Yang, and **C. Coddet,** LERMPS, Institut Polytechnique de Sévenans, BP 449, 90010 Belfort Cedex, France; **P. Vaslin,** UFR STAPS Clermont-Ferrand, BP 104, 63172 Aubere Cedex, France.

2. Experimental Conditions

Spray facilities used in this study were a Plasma-Technik A-2000 console (Sulzer-Metco, Rigackerstrasse 21, 5610 Wohlen, Switzerland) with a PT-F4 gun for plasma spraying and a Plasma-Technik CDS-100 (Sulzer-Metco, Rigackerstrasse 21, 5610 Wohlen, Switzerland) for high-velocity oxygen fuel (HVOF) spraying.

Nomenclature

a	displacement of the top end of the specimen, μm
e	thickness, μm
E	elastic modulus, GPa
K	curvature, m^{-1}
y_0	position of the neutral fiber in the specimen through thickness, μm
y	distance between the point studied and y_o, μm
T	temperature, °C
α	thermal expansion coefficient, $°C^{-1}$
σ	residual stress, MPa
σ_y	yield strength of the substrate material, MPa

Subscript

i	ith layer
s	substrate
m	coating/substrate system
c	coating
g	total
q	quenching
th	thermal
bc	prior to the cooling
ec	end of the cooling
0	room temperature

Specimens used for curvature measurements were 304L stainless steel plates with dimensions 80 mm length by 15 mm width by 1 mm thickness. The elastic modulus of the steel is 200 GPa, and the expansion coefficient is $16 \times 10^{-6}\ °C^{-1}$. Spray parameters are presented in Table 1, and the main characteristics of powders are shown in Table 2.

The specimen was clamped at one end of a cylindrical aluminum drum, 100 mm in diameter (Fig. 1). The other end was not clamped, so the specimen could respond to the stress field generated during the spray process.

The specimen holder was rotated to allow a relative linear speed of the specimen with respect to the torch of 75 m · min^{-1}. Deformation of the specimen on its support during spraying was recorded with a high speed video system (NAC HSV1000; IPI, 24 rue Robert Witchitz, 94200 Ivry Sur Seine Cedex, France) at a recording frequency of 500 frames per second (500 Hz) with a shutter speed of 1/5000 second (Fig. 2).

The video camera was equipped with a 100 mm objective and placed approximately 40 cm from the specimen. In these conditions, the field of view of the camera was: for horizontal axis, L = 16 cm and for vertical axis, H = 12 cm.

Images analysis was performed with an Ariel performance analysis system (APAS), including (a) an S-VHS/NTSC video recorder that reads video bands recorded by the system NAC HSV1000 and (b) a microcomputer AST-PREMIUM II equipped with a video card that uses image digitizing and acquisition of software for data processing.

Displacement measurement of the free end of the specimen was performed only when the specimen surface was perfectly parallel to the camera axis. Considering the high recording frequency and the deflection level of the specimen, only one image per four revolutions of the specimen holder was digitized. The rotation speed of the support was 240 rpm, and because F = 4 Hz, the digitizing frequency of the images was 1 Hz.

This operation was performed manually because the stability of the rotation control (±1 rpm) did not allow automatic selection of the frames.

Two measurement points were set on each digitized image, the top end of the specimen (point D in Fig. 3) and the fixture point of the specimen on the drum (point A). Precision of the measurement was estimated to be about ±150 μm. It was necessary to add an error linked to the theoretical precision of the measurement because of an instability in the rotation speed of the drum. This error led to analyzed images that did not always correspond exactly to the instant when the specimen was perfectly parallel to the camera axis. Therefore, recorded values were smoothed using Cricket Graph III software (Computer Associate).

Curvature "K" was obtained from the value displacement of the free end of the specimen by the following method (Fig. 3). After specimen deformation, it was approximated that the angle ADB is 90° because a is small compared to L. Furthermore, because the specimen deforms homogeneously over all its length AB, the AB arc is a circular arc with a center found in O and a radius of r.

C is the middle of AD, then from simple geometry (angles with two perpendicular sides), triangle AOC is similar to triangle DAB (if specimen deformation is very small), therefore:

$$\frac{DB}{AC} = \frac{AD}{OA}$$

with DB = a, AD = L, AC = $L/2$, and OA = r. Thus:

$$\frac{a}{L/2} = \frac{L}{r}$$

and so:

$$K = \frac{1}{r} = \frac{2a}{L^2}$$

Temperature of the specimen was determined during spraying using an infrared pyrometer. This pyrometer was calibrated before the tests by recording the temperature of a WC/Co coating simultaneously with the pyrometer and a thermocouple. To limit initial emissivity problems, the aluminum drum was entirely covered by a plate of stainless steel.

Table 1 Thermal spraying parameters

	APS1	APS2	HVOF
Ar flow rate, 1 · min^{-1}	47.5	47.5	...
He flow rate, 1 · min^{-1}	170	170	...
O_2 flow rate, 1 · min^{-1}	...	...	420
C_3H_8 flow rate, 1 · min^{-1}	...	...	60
Powder flow rate, g · min^{-1}	40	8 (preheating) 40 (spraying)	48
Preheating	no	yes	yes
Cooling	yes	yes	yes
Tmax, °C	130	160	180
Stand off distance, mm	125	125	300

Table 2 Powders reference and composition

Spraying	Reference	Composition	Size range, μm
APS	Amdry 983	WC 17% + Co	-63
HVOF	Amdry 1983	WC 17% + Co	+11–45

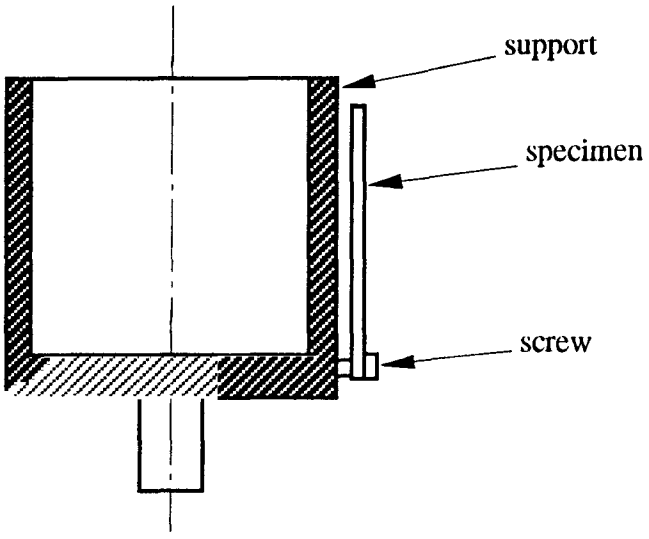

Fig. 1 Specimen holder and setting of the specimens

Increase in coating thickness (*del/dt*) during spraying was also considered to be linear with time, assuming that the deposition rate did not change with time or with specimen temperature.

3. Calculation Procedure

To calculate stress distribution in the coating, the following assumptions were made. (a) Temperature gradient is negligible for a thin specimen. (b) The substrate and the deposit behave as isotropic materials. (c) Two main stress generating factors, quenching stress due to cooling of splats and thermal stress due to the difference in thermal expansion coefficient of the coating and substrate, occur during the spraying.

The coating is formed layer by layer. A layer on the substrate with a temperature T_0 induces quenching stress σ_q. Then, if the temperature of the coating and the substrate increases to T_1, a thermal stress σ_{th} is generated due to the difference in the expansion coefficients between the layer and the substrate. If the temperature remains stable during the spray process, only the quenching stress is considered (Ref 4).

Thus, during spraying, the total stress in the last layer deposited on the substrate is:

$$\sigma_g = \sigma_q + \sigma_{th} \quad \text{(Eq 1)}$$

where σ_g is the total stress, σ_q is the quenching stress, and σ_{th} is the thermal stress. The specimen curvature produced by this layer can be written as:

$$K_g = K_q + K_{th} \quad \text{(Eq 2)}$$

where K_g is the total curvature, K_q is the curvature due to the quenching stress, and K_{th} is the curvature due to the thermal stress. The parameter K_g is measured during the spray process, and K_{th} can be calculated from the evolution of temperature, the thickness of the layer, the expansion coefficients, and the elastic modulus of the layer and the substrate. Therefore, curvature K_q, due to the quenching stress, can also be calculated.

From these boundary conditions, stress was determined by the following method. For the ith and last deposited layer on the substrate, the stresses are:

$$\sigma_{gi} = \sigma_{qi} + \sigma_{thi} \quad \text{(Eq 3)}$$

Applying Stoney's formula (Ref 5) and taking into account the composite structure of the substrate having i–1 layers, the quenching stress can be written as:

$$\sigma_{qi} = \frac{E_{m(i-1)}\left(e_s + \sum_{i=1}^{n} e_{i-1}\right)^2}{6} \frac{\Delta K_{qi}}{e_i} \quad \text{(Eq 4)}$$

and the thermal stress

$$\sigma_{thi} = E_c(\alpha_{mi} - \alpha_c)(T_i - T_{i-1}) + E_c(y - y_0)\Delta K_{thi} \quad \text{(Eq 5)}$$

where e_i is the thickness of the ith layer and ΔK_{thi} is the increase in the curvature of the specimen due to the increase of the temperature. The parameter ΔK_{thi} is obtained from the following equation (Ref 6):

$$\Delta K_{thi} = \frac{6E_{mi}E_c e_{mi} e_i (e_{mi} + e_i)(\alpha_{mi} - \alpha_c)(T_i - T_{i-1})}{E_{mi}^2 e_{mi}^4 + E_c^2 e_i^4 + 2E_{mi}E_c e_{mi} e_i (2e_{mi}^2 + 2e_i^2 + 3e_{mi}e_i)} \quad \text{(Eq 6)}$$

where E_{mi} is the composite elastic modulus of the specimen having i layers that can be calculated according to the law of mixtures, that is:

$$E_{mi} = \frac{E_s e_s + E_c \sum_{i=1}^{n} e_i}{e_s + \sum_{i=1}^{n} e_i} \quad \text{(Eq 7)}$$

where E_s is the elastic modulus of the substrate and E_c is the elastic modulus of the deposit, e_s is the thickness of the substrate, $\sum_{i=1}^{n} e_i$ is that of the deposit, and α_{mi} is the expansion coefficient of the composite specimen, which can also be calculated using the same principle:

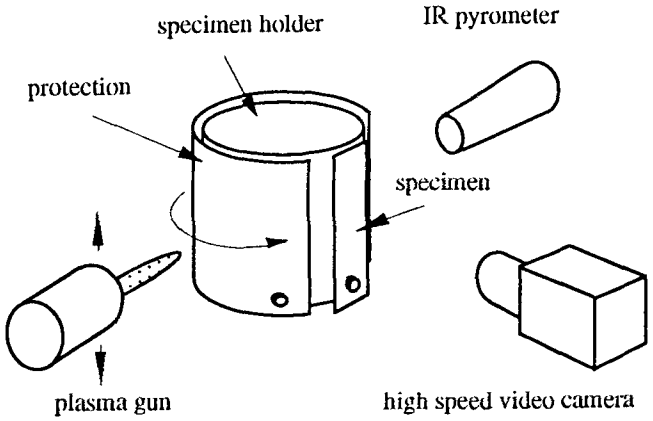

Fig. 2 Setting for the in situ measuring of the specimen deformation

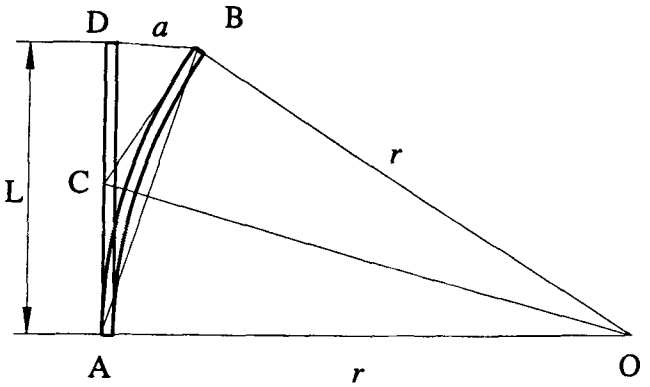

Fig. 3 Geometric relationships in the curvature system

$$\alpha_{mi} = \frac{E_s e_s \alpha_s + E_c \sum_{i=1}^{n} e_i \alpha_c}{E_s e_s + E_c \sum_{i=1}^{n} e_i} \quad \text{(Eq 8)}$$

with α_c and α_s being the expansion coefficients, respectively, of the layer and the substrate.

If y_o is the position of the neutral fiber, and y is the distance between this position and the point where the stresses are calculated, as shown in Fig. 4, their values can be calculated using the following equation:

$$y_{oi} = \frac{E_s e_s^2 - E_c \left(\sum_{i=1}^{n} e_i \right)^2}{2 \left(E_s e_s + E_c \sum_{i=1}^{n} e_i \right)} \quad \text{(Eq 9)}$$

$$y = - \sum_{i=1}^{n} e_i \quad \text{(Eq 10)}$$

This calculation is only suitable for the ith layer at the moment when it is the last layer. With the occurrence of successive layers, the stresses in the former layers are modified.

For example, when the jth layer is formed, the stress in the first layer becomes:

$$\sigma_{1,j} = \sigma_1 + \sigma_{j \to 1} \quad \text{(Eq 11)}$$

where $\sigma_{j \to 1}$ is the increase of stress in the first layer due to the jth layer. This increase can be expressed according to the following equation:

$$\sigma_{j \to 1} = E_c(\alpha_{mj} - \alpha_c)(T_j - T_{j-1}) + E_c(-e_1 - y_{0j})(K_{gj} - K_{gj-1}) \quad \text{(Eq 12)}$$

Similarly for the ith layer, the same calculation can be performed:

$$\sigma_{i,j} = \sigma_i + \sigma_{j \to 1} \quad \text{(Eq 13)}$$

with

$$\sigma_{j \to i} = E_c(\alpha_{mj} - \alpha_c)(T_j - T_{j-1}) + E_c(-e_i - y_{0j})(K_{gj} - K_{gj-1}) \quad \text{(Eq 14)}$$

Stress in the substrate was calculated by assuming that it deformed independently from the coating under the action of the stress in the coating. According to the specimen curvature, this stress can be determined by considering that the substrate material is not work hardenable. When the calculated stress exceeds the yield strength of the material, the level of stress is considered equal to the yield strength; the substrate thickness is correspondingly reduced to take into account the plastic deformation.

Thus, stresses in the coating are calculated within the elastic limit of the material with a substrate thickness that is artificially decreased when plastic deformation appears in the substrate to keep the maximum stress level equal to the level of the yield strength.

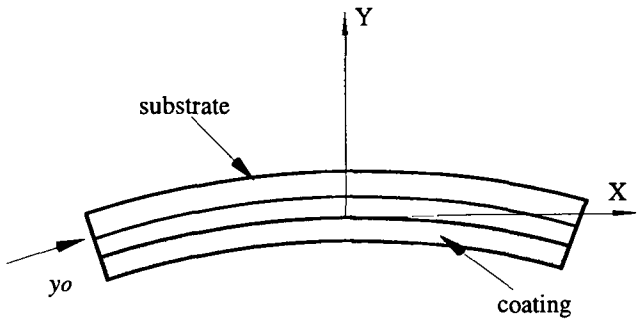

Fig. 4 Definition of y and y_0

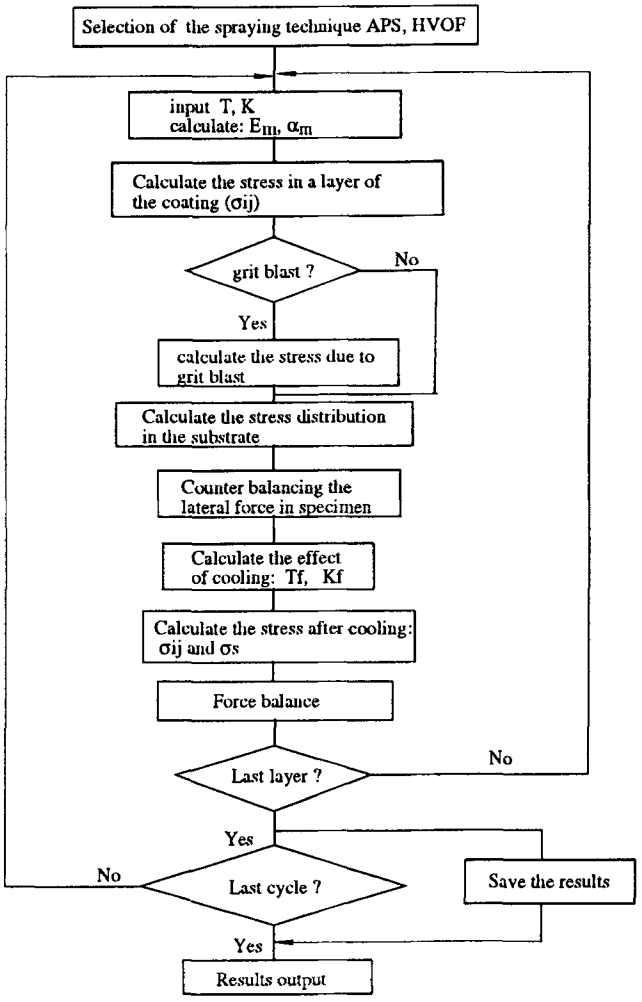

Fig. 5 Computer program flow chart

Therefore, calculations are performed according to the following sequence: (1) determination of the stress in the substrate due to ΔK; (2) determination of the totality of lateral forces in the substrate; (3) balancing lateral forces in the substrate with those of deposited layers; and (4) calculation of the equivalent elastic thickness of the substrate by comparing the stress at each point of thickness with the yield strength σ_y.

After spraying, the specimen enters the cooling period that again produces a modification of the stress level and a partition between the coating and the substrate. The cooling stress in the coating can be expressed as:

$$\sigma_{cr} = E_c(\alpha_m - \alpha_c)(T_{ec} - T_{bc}) + E_c(y - y_0)(K_{ec} - K_{bc}) \quad \text{(Eq 15)}$$

and in the substrate by:

$$\sigma_{sr} = E_s(\alpha_m - \alpha_s)(T_{ec} - T_{bc}) + E_s(y - y_0)(K_{ec} - K_{bc}) \quad \text{(Eq 16)}$$

where T_{ec} and T_{bc} are, respectively, the temperature at the end of cooling and prior to cooling, and where K_{ec} and K_{bc} are, respectively, the curvature at the end of cooling and prior to cooling.

Final stress distribution is expressed in the coating by:

$$\sigma_{cf} = \sigma_{cr} + \sigma_c \quad \text{(Eq 17)}$$

and in the substrate by:

$$\sigma_{sf} = \sigma_{sr} + \sigma_s \quad \text{(Eq 18)}$$

Software was written on the basis of the above-described procedure to calculate the stress (Fig. 5).

The initial grit blasting also generates stresses in the substrate (Ref 7), which influences the calculation because the superposition of stresses brings the substrate into the plastic zone. In this work, the stress caused by grit blasting was measured by the curvature method by gradually reducing the thickness of the specimen with chemical etching (Fig. 6). This stress state was considered the original state of the sample for later stress calculations in the substrate during the spraying.

Centrifugal force produced by rotation of the specimen may also induce a small deflection of the plate. A calculation, according to the beam theory of mechanics, gives maximal displacement of the free end of the specimen of about 500 μm without the coating and 400 μm with a coating thickness of 300 μm. To ease the calculations, all measurements were corrected according to these data to eliminate the influence of the centrifugal force on the stress determination.

In all calculations, the elastic modulus of the WC/Co coating was estimated at 150 GPa (Ref 8), and assuming minimal difference between a massive material and the coating (Ref 9), the expansion coefficient was taken as 5×10^{-6}/ °C (Ref 10).

4. Results and Discussion

This study focused on three different thermal spraying conditions: (a) APS1, four successive spraying sequences (50, 90, 90, and 80 s); (b) APS2, one sequence of 330 s duration; and (c) HVOF, one sequence of 300 s duration.

For specimen APS1, strong air jet cooling was chosen to minimize the specimen average temperature. When the temperature reached 130 °C, spraying was interrupted to allow the specimen to cool (Fig. 7). It was observed that four cycles occurred during the spray procedure and that between the cycles, the specimen was cooled to about 30 °C for one minute.

Three steps can be considered in the evolution of specimen curvature during each cycle (Fig. 8). (a) At the beginning of the spraying, the curvature increases rapidly, with the temperature. (b) After a certain period of time, the curvature evolution is almost linear, and temperature of the specimen is almost stable. (c) At the end of the cycle, the curvature decreases because the specimen temperature falls rapidly.

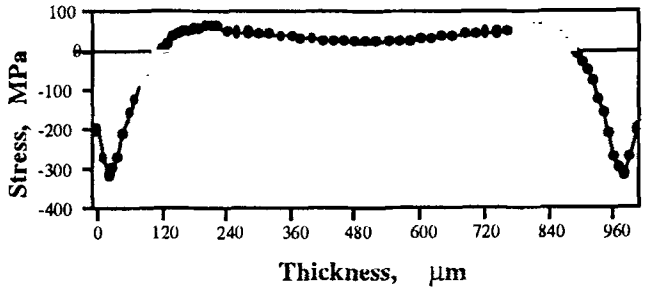

Fig. 6 Distribution of stress in the substrate, which is sand blasted on two sides

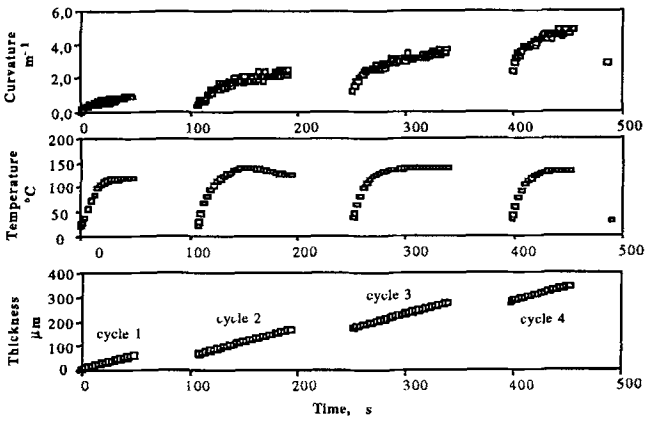

Fig. 7 Evolution of the curvature, temperature, and coating thickness as a function of time for APS1. (During cooling between cycles, the deflection of the specimen was not recorded.)

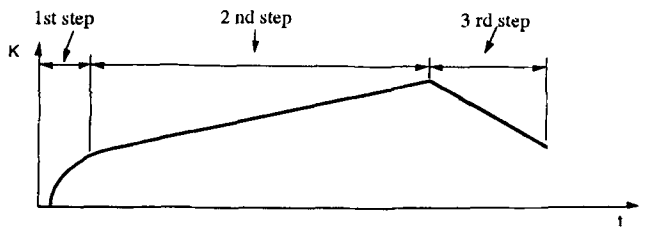

Fig. 8 Evolution of the specimen curvature as a function of time (schematic only)

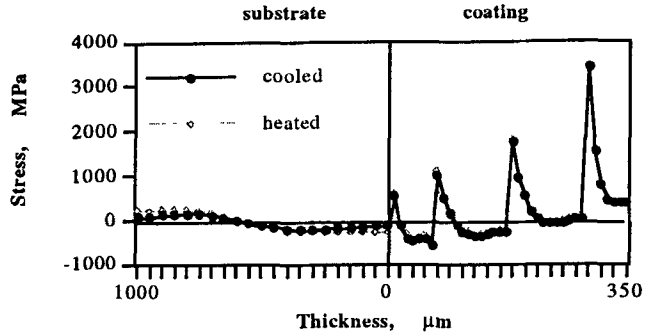

Fig. 9 Distribution of stress in the coating and the substrate for APS1 (heated, after spraying; cooled, after cooling)

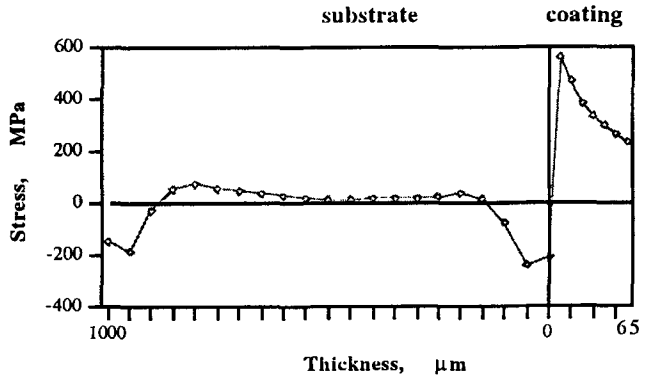

(a)

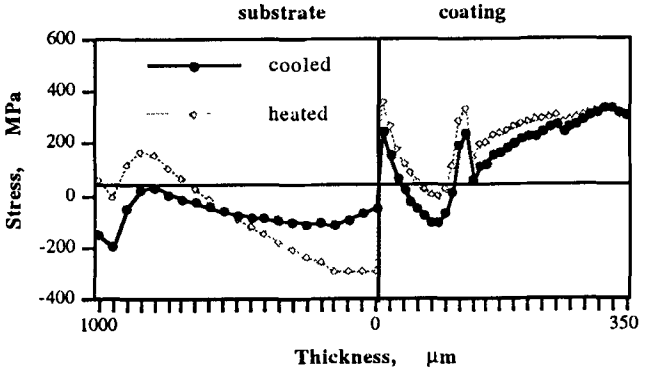

(b)

Fig. 11 Stress distribution in the specimen APS2 (a) after the preheating period, and (b) at the end of spraying (heated) and the end of cooling (cooled)

Calculated stress evolution of APS1 is shown in Fig. 9, which indicates the stress distribution after four cycles. Stress increases rapidly at the beginning of the cycle and then decreases during spraying within a given cycle. It is noted that stress in the substrate is not homogeneous because the elastic deformation limit is exceeded during the spray procedure.

Specimen APS2 was preheated, and a small amount of powder was sprayed to protect the substrate from oxidizing. The evolution of specimen curvature, temperature, and thickness, as a function of time, is shown in Fig. 10. Deposition rate changed at 120 s (0.48 μm/s before and 1.28 μm/s after) by adjusting the

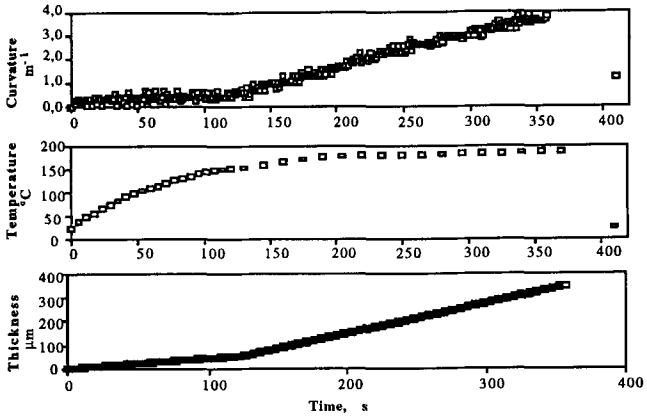

Fig. 10 Evolutin of the curvature, the temperature, and the coating thickness as a function of time for APS2

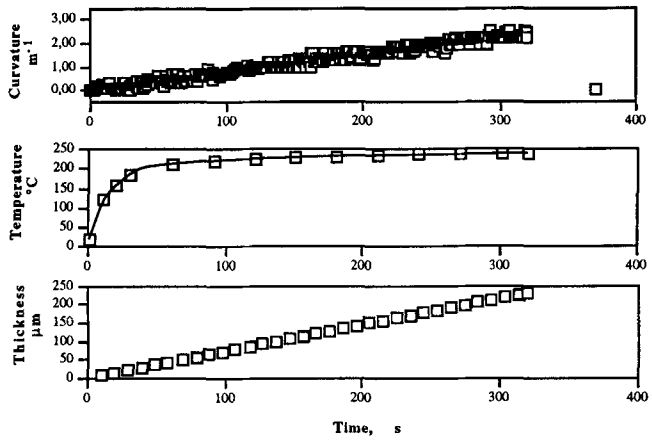

Fig. 12 Evolution of the curvature, the temperature, and the coating thickness as a function of time for the high-velocity oxygen fuel (HVOF) spraying

powder feed rate. The increase in the specimen temperature was much slower than that for APS1 due to the lower initial powder feed rate.

Three steps are also observed with regard to the evolution of curvature. In the first step, when spraying begins, the curvature increases slowly because the powder feed rate is low. After temperature stabilization, around 150 °C, the powder feed rate was increased, and the curvature started to increase linearly, showing the effect of the deposition alone, which was nearly independent of the temperature.

The corresponding stress evolution is shown in Fig. 11. Overall, stresses are lower for APS2 than for specimen APS1, and they are more homogeneous. From these results, it appears that preheating can decrease the stress level in the coating, especially at the coating/substrate interface.

Figure 12 shows the evolution of temperature, curvature, and coating thickness for HVOF spraying. Prior to powder feeding, a short preheating period (10 s) rapidly increases the substrate temperature to ~100 °C.

During spraying, the temperature remained relatively stable but rather high (210 °C) compared to the APS spraying. The evolution of curvature as a function of time is slow and nearly linear.

Final curvature after cooling is almost zero (0.011/m). The calculated stress distribution in the coating is shown in Fig. 13. Average stress is almost identical to that of specimen APS2, in spite of lower curvature. In fact, the rate change of the curvature determines the stress level more than the final curvature.

Results show that at the beginning of spraying, stress increases rather rapidly in all cases due to the rapid increase of the substrate temperature and to the difference in the expansion coefficients between the coating and the substrate. At this period, the thermal effect is the dominant factor in stress generation.

During spraying, stresses in the coating are tensile and higher than after cooling. A higher temperature during spraying induces greater stress reduction after spraying because the substrate contracts more than the coating during the cooling period (that is, the expansion coefficient of the substrate is greater than that of the coating). Once the temperature and the powder feed rate are stable, the stress increase in the coating is almost linear. This confirms that the quenching stress is always tensile, and it increases regularly if the temperature is stable.

5. Conclusions

Temperature history of the specimen during spraying plays an important role in the level and distribution of residual stresses in the coating, particularly when the difference in the value of expansion coefficient is important.

Preheating of the specimen decreases the stress in the coating by counter balancing the difference in the expansion coefficients. Preheating with a small powder feed rate improves the stress distribution, especially at the interface, and increases the adhesion of the deposit to the substrate by reducing the interfacial stress.

Continuous increase of the quenching stress with the increase of the coating thickness under typical spray conditions demonstrates the need for thickness limitations during thermal spraying.

Acknowledgment

The authors thank the CRIPS (Center for Products Design) for use of the high speed video camera.

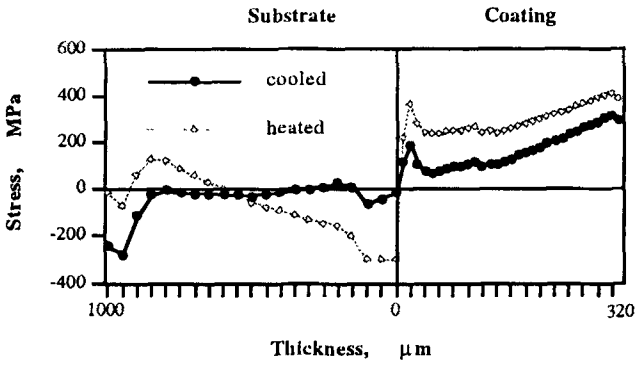

Fig. 13 Distribution of stress in the coating and in the substrate for the HVOF specimen

References

1. R. Knight and R.W. Smith, Residual Stress in Thermally Sprayed Coatings, *Thermal Spray Coatings: Research and Application,* C.C. Berndt and T.F. Bernecki, Ed., ASM International, 1993, p 607-612
2. W.J. Lenling, M.F. Smith, and J.A. Henfling, Beneficial Effects of Austempering Post-Treatment on Tungsten Carbide Based Wear Coating, *Thermal Spray Research and Applications,* T.F. Bernecki, Ed., ASM International, 1990, p 227-232
3. S.C. Gill and T.W. Clyne, Stress Distributions and Material Response in Thermal Spraying of Metallic and Ceramic Deposits, *Metall. Trans. B,* Vol 21, April 1990, p 377-385
4. S. Kuroda and W. Clyne, The Quenching Stress in Thermally Sprayed Coatings, *Thin Solid Films,* 200, 1991, p 49-66
5. G. Stoney, The Tension of Metallic Layers Deposited by Electrolysis, *Proc. R. Soc. (London),* Vol A82, 1909, p 172-175
6. C.H. Hsueh and A.G. Evans, Residual Stresses in Metal/Ceramic Bonded Strips, *J. Am. Ceram. Soc.,* Vol 1 (No. 5), 1985, p 24-48
7. S. Kuroda, T. Fukushima, and S. Kitahara, Generation Mechanisms of Residual Stresses in Plasma-Sprayed Coatings, *Vacuum,* Vol 41 (No. 4-6), 1990, p 1297-1299
8. C. Richard, "Etude des Caractéristiques Mécaniques de Revêtements Projetés par Procedés Thermique" (Studies on the Mechanical Characteristics of the Coatings Thermally Sprayed), thesis, Université de Technologie de Compiègne, 1992 (in French)
9. S.C. Gille, "Residual Stress in Plasma Sprayed Deposits," thesis, University of Cambridge, 1991
10. Y. Coutial, "Etude du Comportement Mécanique à Haute Température de Cermet WC/Co—Effet de la Microstructure," (Studies on the Mechanical Behavior of the WC/Co Cermet Coating at High Temperature—The Effect of Microstructure), thesis, I.N.S.A., Nov 1991 (in French)